Supplementary Information

Thickness-dependent response of aerosol-jet-printed ultrathin high-aspect-ratio electrochemical microactuators

Ji Zhang,[ab] Jeremy J. Baumberg*[b] and Sohini Kar-Narayan*[a]

[a] *Department of Materials Science & Metallurgy, University of Cambridge, 27 Charles Babbage Road, Cambridge CB3 0FS, UK. E-mail: sk568@cam.ac.uk*

[b] *NanoPhotonics Centre, Cavendish Laboratory, University of Cambridge, JJ Thomson Avenue, Cambridge CB3 0HE, UK. E-mail: jjb12@cam.ac.uk*

Table S1. Printing parameters for each ink

		PEDOT:PSS	**Nafion**	**Nafion encapsulation**	**Au**
Atomiser		Ultrasonic	Pneumatic	Pneumatic	Ultrasonic
Atomiser current		~0.6 A	n/a	n/a	~0.6 A
Bubbler		DI water	Ethanol	Ethanol	DI water
Nozzle size		300 µm			
Ambient temperature		~20 °C			
Platen temperature		80 °C			
Chiller temperature		20 °C	n/a	n/a	20 °C
Sheath flow rate		140 sccm	140 sccm	140 sccm	140 sccm
Ink flow rate†		30-50 sccm	520-550 sccm	500-520 sccm	15-23 sccm
Exhaust flow rate†		n/a	440-480 sccm	450-460 sccm	n/a
Printing speed		5 mm/s	5 mm/s	5 mm/s	5 mm/s
Raster line separation		20 µm	20 µm	40 µm	20 µm
No. of printing passes	Varying PEDOT:PSS thickness	1, 2, 3, 4, 5, 6	8	1	2
	Varying Nafion thickness	2	5, 8, 11, 14, 17, 20	1	2
	Varying actuator length	2	8	1	2
Curing condition		150 °C, 2 hours			

†The ink and exhaust flow rates are sometimes slightly adjusted to compensate for the change in appearance of aerosol deposition over time.

n/a: Not applicable; sccm: standard cubic centimetres per minute

Fig. S1. Three PEDOT:PSS/Nafion/PEDOT:PSS actuator designs without incorporation of Au contact electrodes.

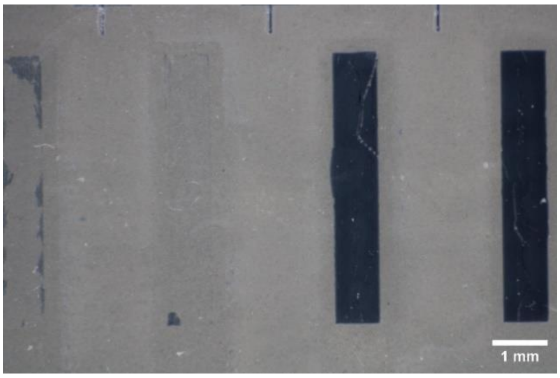

Fig. S2. Leftover bottom layer PEDOT:PSS after actuators (design A in **Fig. S1**) with different PEDOT:PSS thicknesses are peeled off. Left to right: 1 printing pass, 2 printing passes, 3 printing passes, and 4 printing passes.

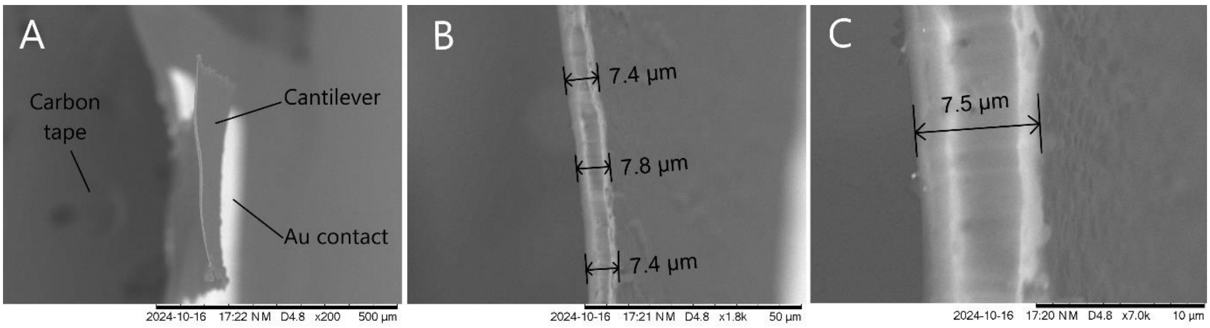

Fig. S3. SEM cross-sectional images of actuator with 4 PEDOT:PSS printing passes, taken at different magnifications.

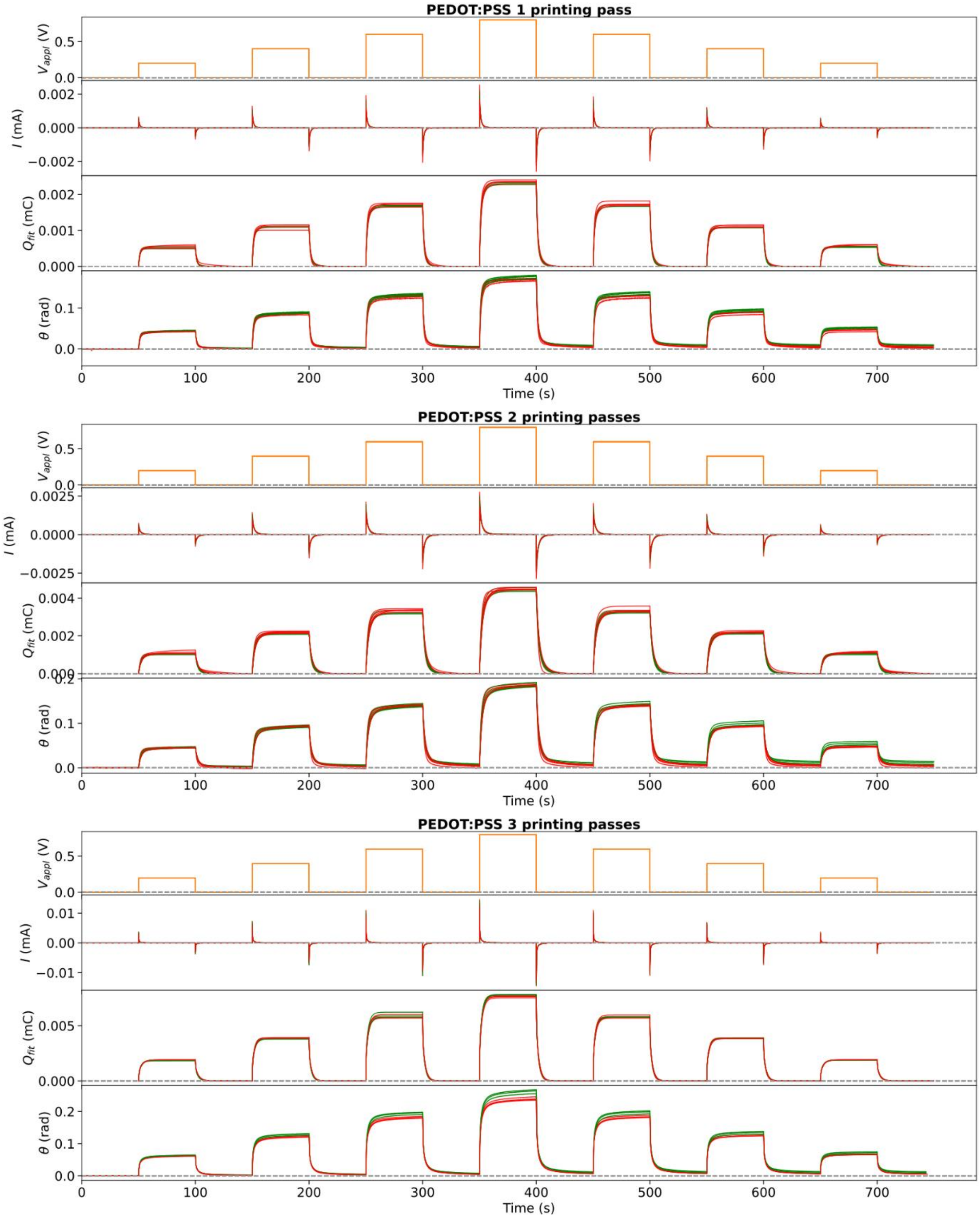

Fig. S4. Voltage, current, fitted charge, and deflection over time for DC actuation tests with varying PEDOT:PSS thicknesses. The red and green curves indicate voltage applied in both directions.

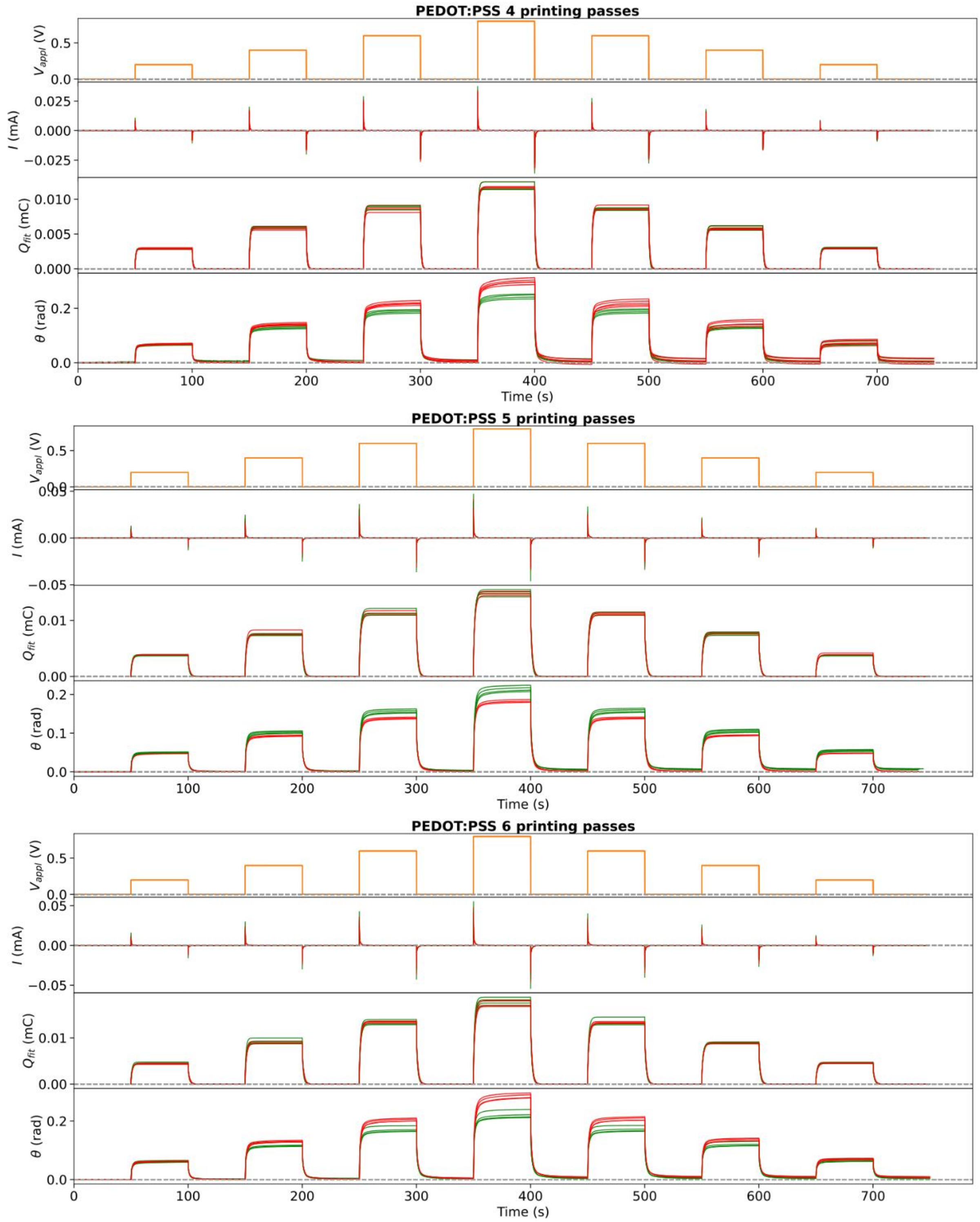

Fig. S4 (cont'd). Voltage, current, fitted charge, and deflection over time for DC actuation tests with varying PEDOT:PSS thicknesses. The red and green curves indicate voltage applied in both directions.

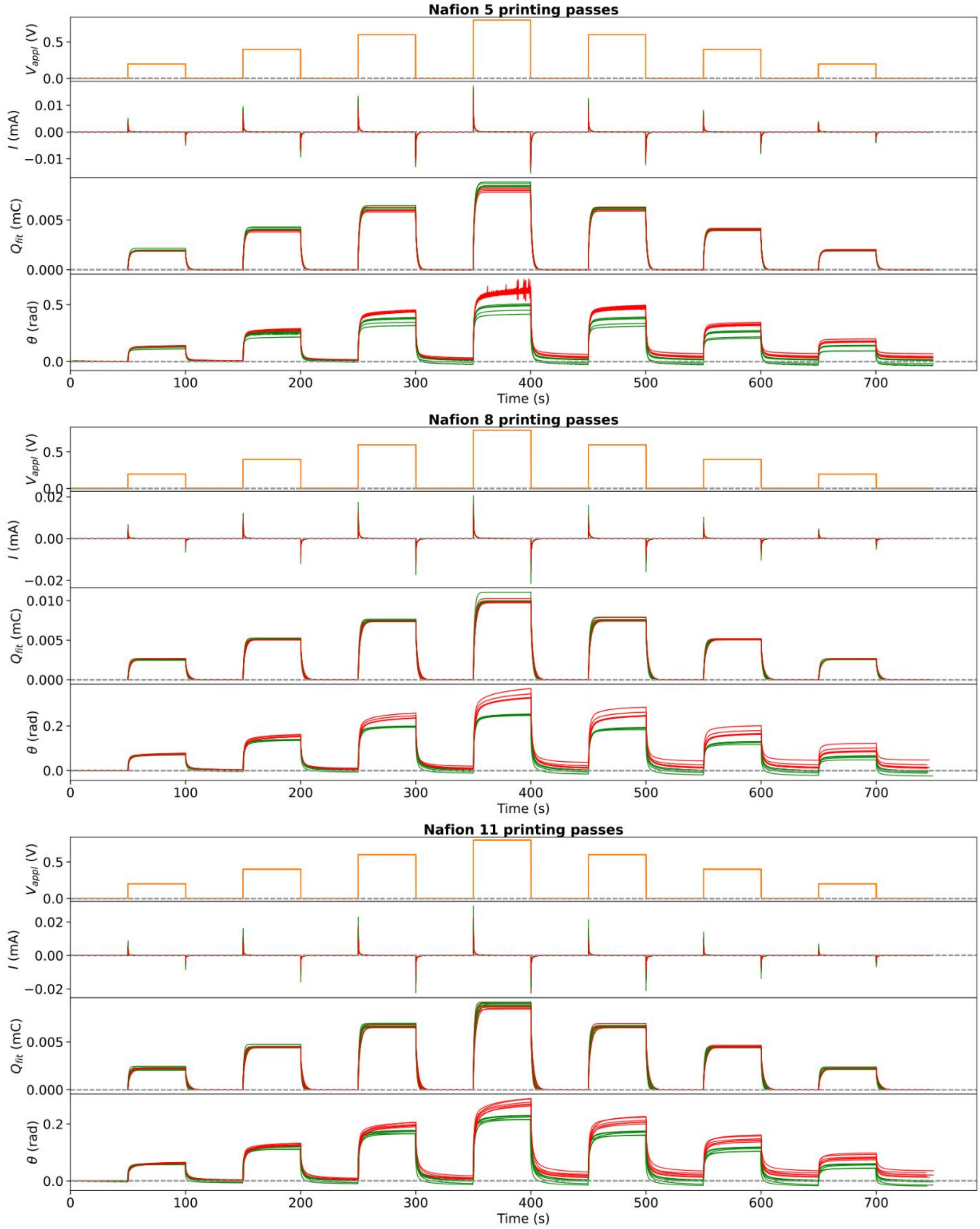

Fig. S5. Voltage, current, fitted charge, and deflection over time for DC actuation tests with varying Nafion electrolyte thicknesses. The red and green curves indicate voltage applied in both directions.

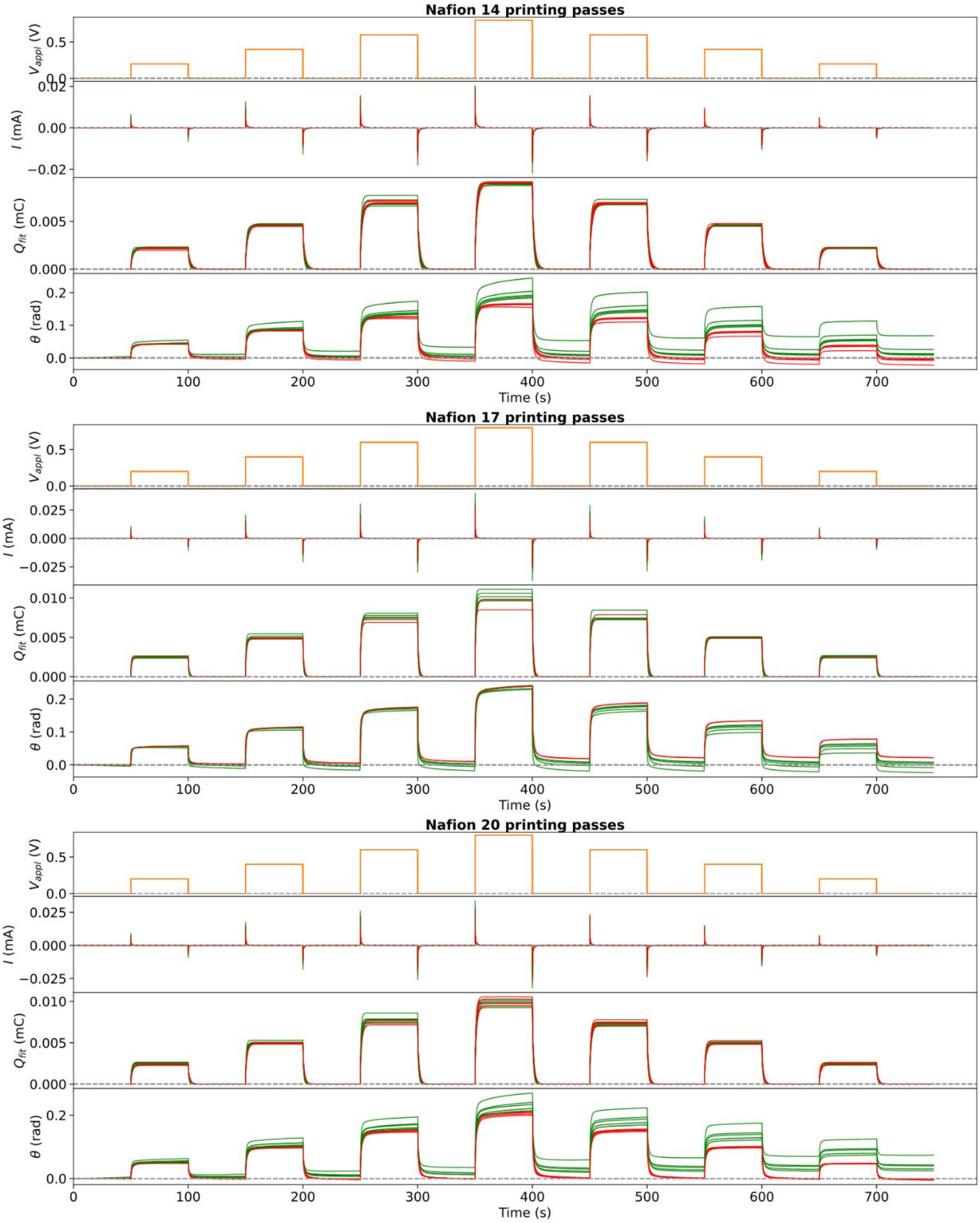

Fig. S5 (cont'd). Voltage, current, fitted charge, and deflection over time for DC actuation tests with varying Nafion electrolyte thicknesses. The red and green curves indicate voltage applied in both directions.

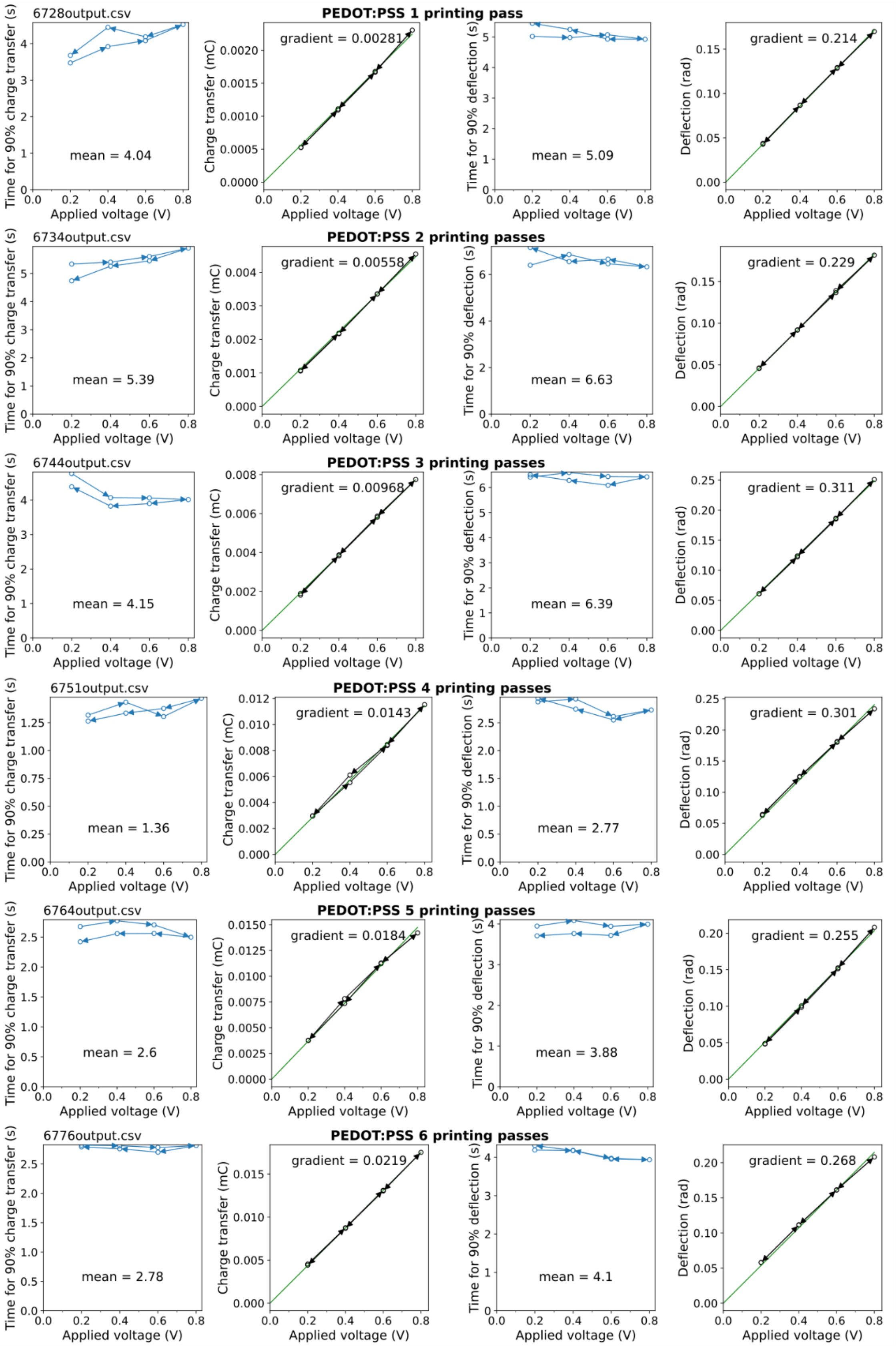

Fig. S6. Examples of actuation test analysis showing the dependence of steady-state charge transfer, steady-state deflection, and time to reach 90% of charge transfer/deflection on applied voltage for actuators with varying PEDOT:PSS thicknesses.

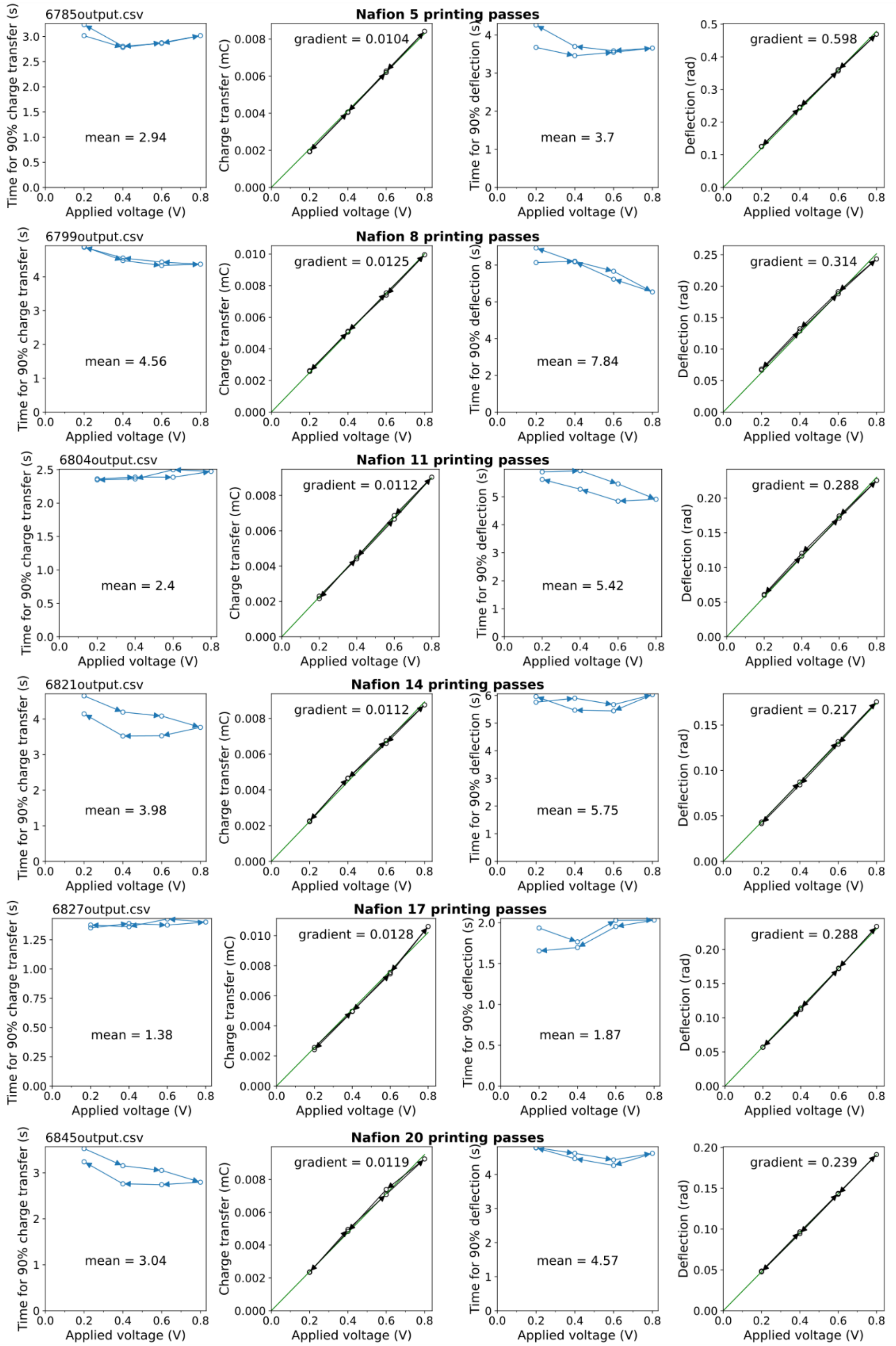

Fig. S7. Examples of actuation test analysis showing the dependence of steady-state charge transfer, steady-state deflection, and time to reach 90% of charge transfer/deflection on applied voltage for actuators with varying Nafion electrolyte thicknesses.

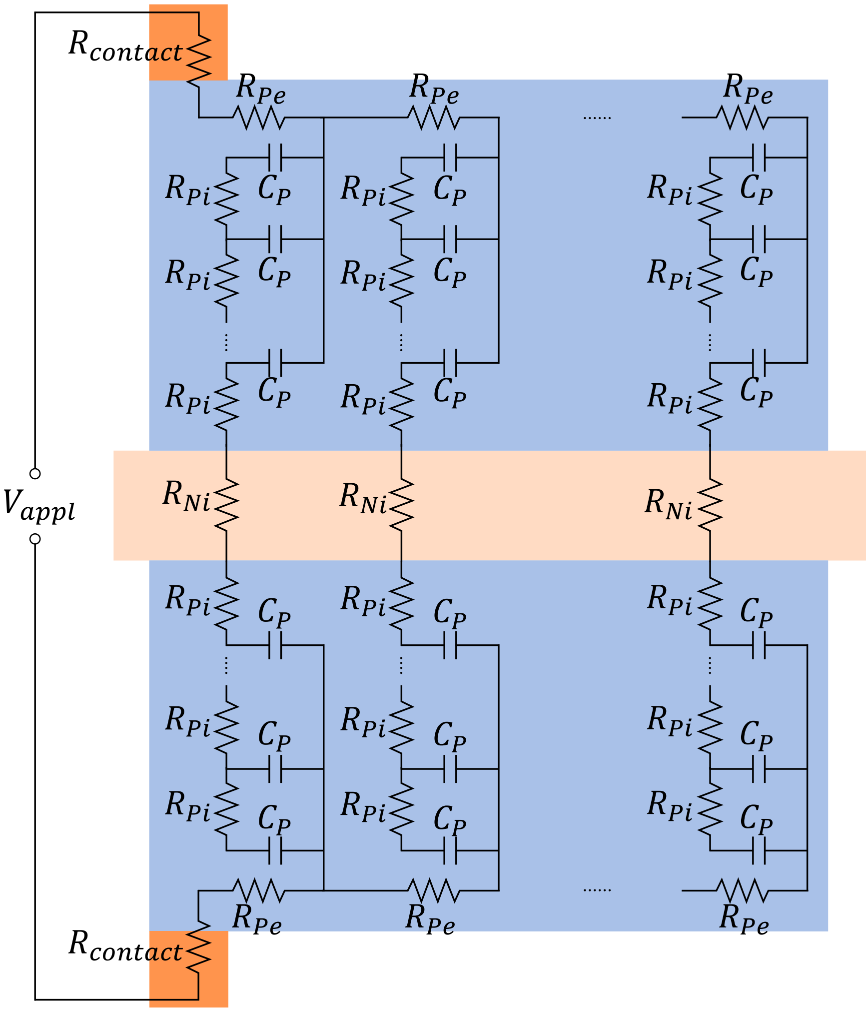

Fig. S8. Transmission line model of trilayer actuator.[1–5] The circuit elements R_{Pi}, R_{Pe}, and C_P represent ionic resistance, electronic resistance and capacitance of small sections in PEDOT:PSS; R_{Ni} represents ionic resistance across portions of the Nafion electrolyte; $R_{contact}$ represents the contact resistance. At steady state, the currents in all branches of the circuit are zero; thus, the electric potential only drops across the capacitors. Assuming uniform thicknesses and material properties of PEDOT:PSS along the length of the actuator, the potential in the Nafion electrolyte layer would be the same along the actuator. Hence, the capacitors in each PEDOT:PSS electrode can be combined and treated as one capacitor.

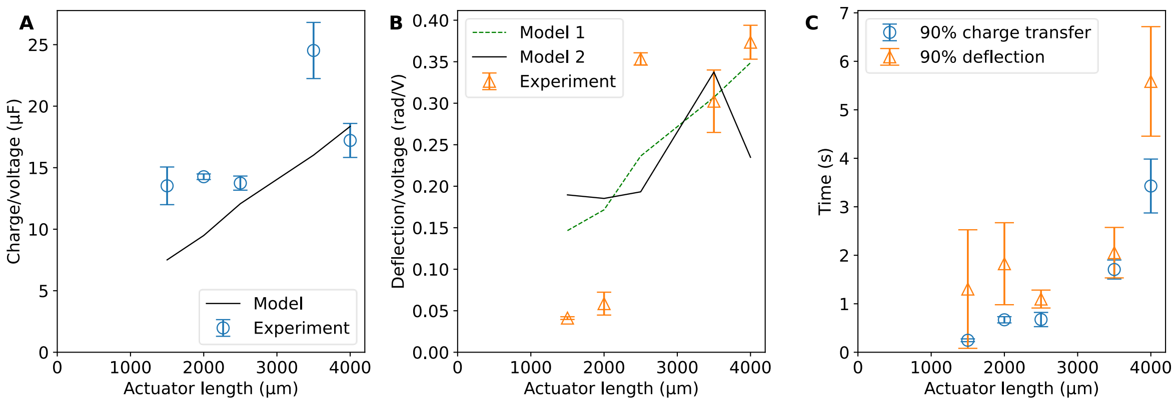

Fig. S9. (A) Charge-to-voltage ratio, **(B)** deflection-to-voltage ratio, and **(C)** time taken to reach 90% charging and 90% deflection for actuator samples with different lengths. The modelling results in (A) and (B) are discrete points with the same x-values as the experiment data but are connected with lines for visualisation. Error bars for all plots indicate standard deviation of data points with Bessel's correction.

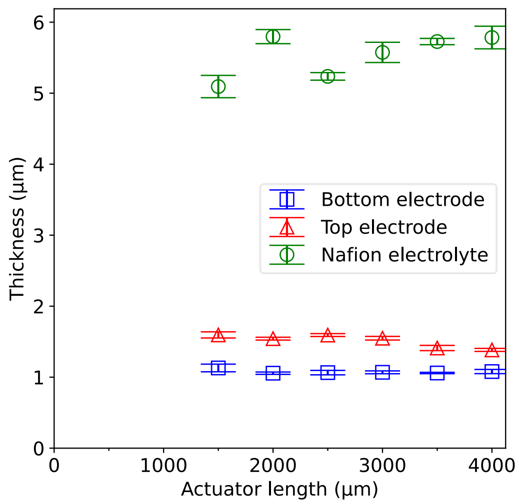

Fig. S10. Thicknesses of PEDOT:PSS and Nafion against number of printing passes in 6 actuator samples with length variation. The error bars indicate standard deviation of results from 4 profilometry scans with Bessel's correction.

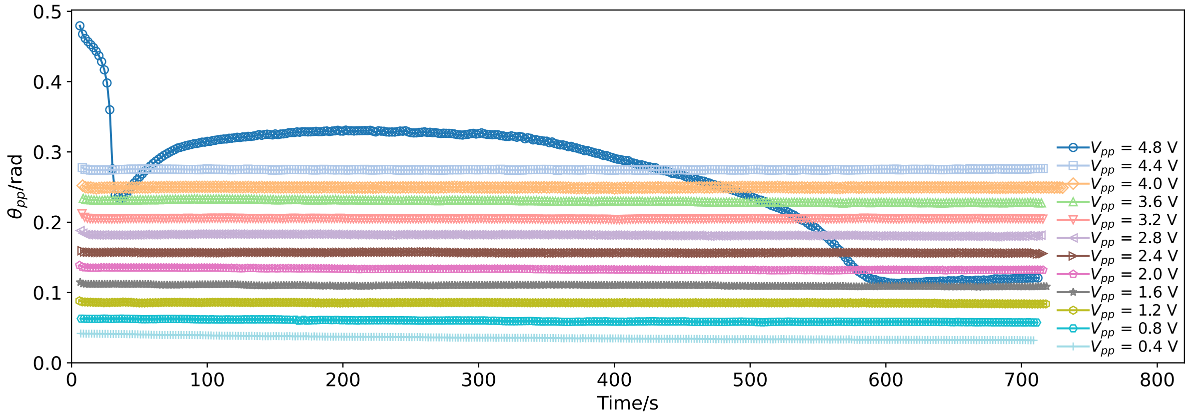

Fig. S11. Durability tests (of the actuator with 4 PEDOT:PSS printing passes) under sine waves at 0.5 Hz, for peak-to-peak voltages from 0.4 V to 4.8 V. Actuation showed minimal deterioration for more than 360 cycles for each voltage until the peak-to-peak voltage reached 4.8 V.

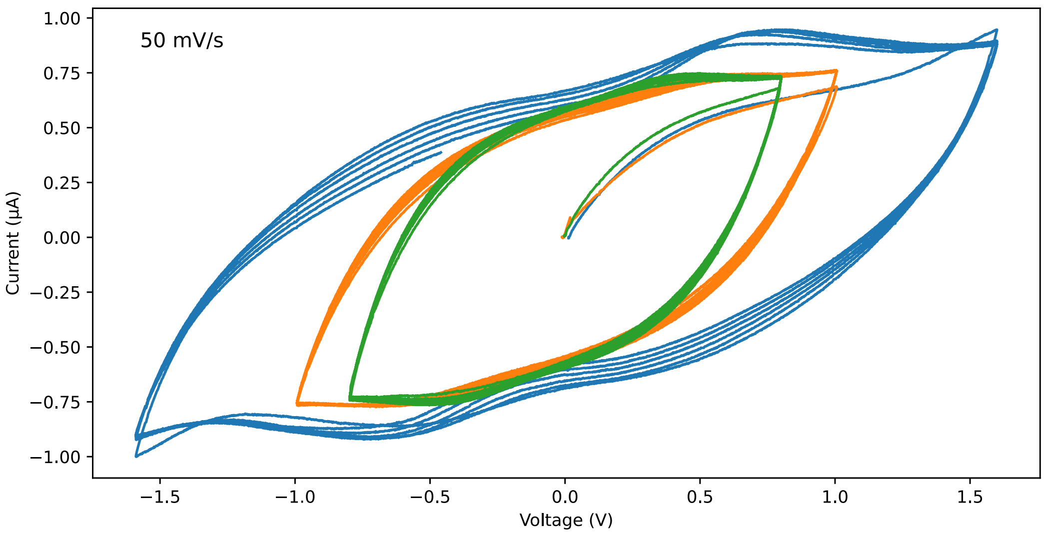

Fig. S12. Cyclic voltammograms (of the actuator with 4 PEDOT:PSS printing passes) measured at 50 mV s^{-1} scan rate between ±0.8 V, ±1 V, and ±1.6 V.

References

1 S. E. Takalloo, H. Seifi and J. D. W. Madden, in *Electroactive Polymer Actuators and Devices (EAPAD) 2017*, SPIE, 2017, vol. 10163, pp. 186–197.
2 T. Shoa, J. D. Madden, C. W. E. Fok and T. Mirfakhrai, *Advances in Science and Technology*, 2008, **61**, 26–33.
3 M. R. Warren and J. D. Madden, *Journal of Electroanalytical Chemistry*, 2006, **590**, 76–81.
4 T. Shoa, D. S. Yoo, K. Walus and J. D. W. Madden, *IEEE/ASME Transactions on Mechatronics*, 2011, **16**, 42–49.
5 F. Bonafè, C. Dong, G. G. Malliaras, T. Cramer and B. Fraboni, *ACS Appl. Mater. Interfaces*, 2024, **16**, 36727–36734.